Research Article Adv. Mater. Lett. 2015, **6**(9), 768-773 Advanced Materials *Letters*

www.amlett.com, www.vbripress.com/aml, DOI: 10.5185/amlett.2015.5888 Published online by the VBRI Press in 2015

A comparative study of polyurethane nanofibers with different patterns and its analogous nanofibers containing MWCNTs

Javier Macossay[1*], Faheem A Sheikh[1, 2, 3 *], Hassan Ahmad[1], Hern Kim[2], Gary L Bowlin[4]

[1]*Department of Chemistry, The University of Texas-Pan American, 1201 W. University Dr., Edinburg TX 78539, USA*
[2]*Nano-Bio Regenerative Medical Institute, College of Medicine, Hallym University, Chuncheon 200-702, South Korea*
[3]*Energy and Environment Fusion Technology Center, Department of Energy and Biotechnology, Myongji University, Yongin, Kyonggi-do 449-728, South Korea*
[4]*Department of Biomedical Engineering, The University of Memphis, Memphis TN 38152, USA*

[*]Corresponding author. Tel.: (+956) 665-3377; E-mail: jmacossay@utpa.edu (J. Macossay); Tel.: (+82) 10-7264-0315, Email: faheem99in@yahoo.com (F.A. Sheikh)

Received: 12 February 2015, Revised: 26 May 2015 and Accepted: 29 May 2015

ABSTRACT

Tissue engineering is a multidisciplinary field that has evolved in various dimensions in recent years. One of the main aspects in this field is the proper adjustment and final compatibility of implants at the target site of surgery. For this purpose, it is desired to have the materials fabricated at the nanometer scale, since these dimensions will ultimately accelerate the fixation of implants at the cellular level. In this study, electrospun polyurethane nanofibers and their analogous nanofibers containing MWCNTs are introduced for tissue engineering applications. Since MWCNTs agglomerate to form bundles, a high intensity sonication procedure was used to disperse them, followed by electrospinning the polymer solutions that contained these previously dispersed MWCNTs. Characterization of the produced nanofibers has confirmed production of different non-woven mats, which include random, semi-aligned and mostly aligned patterns. A simultaneous and comparative study was conducted on the nanofibers with respect to their thermal stability, mechanical properties and biocompatibility. Results indicate that the mostly aligned nanofibers pattern presents higher thermal stability, mechanical properties, and biocompatibility. Furthermore, incorporation of MWCNTs among the different arrangements significantly improved the mechanical properties and cell alignment along the nanofibers. Copyright © 2015 VBRI Press.

Keywords: Nanomaterials; electrospinning; nanofibers; implant; scaffolds.

Introduction

Cells are regulated by the environment that surrounds them, so the type of extracellular matrix (ECM) present will play an important and critical role in providing the structural support needed to reside and grow, thus affecting cell behavior. The ECM consists of a network of nano- and microfibers made up of proteins and glycosaminoglycans, which cross-link in such a way to form a natural scaffold. It is also believed that cells can preferably attach and proliferate in the presence of fibers with diameters smaller than the size of the cells [**1**]. In recent years, tissue engineering has gained tremendous attention due to exciting results in which artificial scaffolds have been used [**2**]. However, the scientific community is still facing major challenges in the formation of new tissue for patients that suffer from various tendon and ligament defects. For this purpose, different materials and designs to fabricate biocompatible scaffolds that present biomechanical properties similar to that of native tissue are still under investigation. Generally, ideal scaffolds for tissue engineering purposes should provide porous architecture for cell seeding, to facilitate host tissue interaction, and for proper vascularization of new tissue [**3, 4**].

A simple experimental setup to produce polymeric nanofibers by using high electric charges was patented by Formhals in 1934 [**5**]; he continued to work in this area, obtaining additional patents on the fabrication of cellulose derivatives fibers [**6-9**]. Gradually, this process started gaining attention in the late 1960s, when Taylor published papers on the disintegration of water droplets and the use of electrically driven jets [**10, 11**]. Electrospinning involves the use of a high voltage to charge the surface of a polymer solution droplet, which becomes unstable and forms what is called a Taylor cone. The charge on the droplet promotes solvent evaporation, leaving behind a polymer fiber charged on its surface, which in turn causes the fiber to stretch and to form continuous and ultrathin fibers that are collected on a grounded collector (**Scheme 1**) [**12-14**]. The fibers obtained through this technique form non-woven structures at the macroscopic level that resemble films, but

microscopically present diameters at the micron and nano scale. The main important feature of this technique is that the morphology of the obtained fibers resembles the structure and dimensions present in natural ECM [**15**]. Moreover, the large surface area of the nanofibers and the high porosity of the electrospun nanofiber mats make them ideal candidates for cell seeding and proliferation for tissue engineering purposes.

Polyurethanes are a family of commercially available polymers [**16**] that have been used in biomedical applications since the 1960's [**17, 18**]. Proper selection of the material permits the formation of fibers that are biocompatible, mechanically strong, and present a low Young's modulus [**19**], which are properties that could be desirable for some tissue engineering applications, such as in ligaments and tendons. Furthermore, multiwalled carbon nanotubes (MWCNTs) are nanomaterials consisting of C-C sp^2 bonds, which result in strong covalent bonds and a hexagonal network that is capable of distortions for relaxing stress [**20-24**], thus possessing high strength and flexibility [**25-28**]. In addition, MWCNTs have been reported to be biocompatible after removal of residual amorphous carbon and catalyst impurities [**29, 30**], so it is expected that addition of these nanomaterials will enhance the mechanical properties of the polymer nanofibers without affecting their biocompatibility.

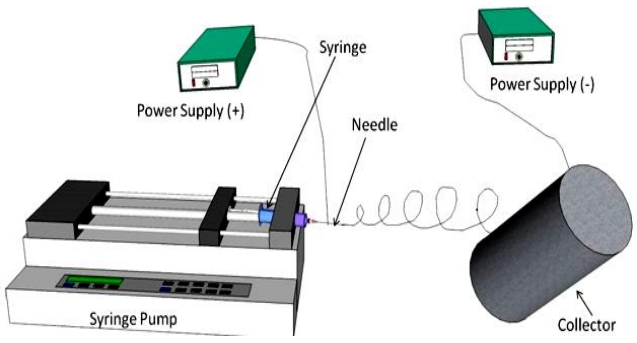

Scheme 1. Simple electrospinning setup used to prepare randomly aligned, semi-aligned and mostly aligned nanofibers.

This manuscript discusses the formation of nanofibers using a biocompatible and non degradable polymer, which could potentially be used in tissue engineering applications. Most of the work being developed in this field uses biodegradable polymers [**14, 31-33**], which might lose their mechanical integrity before the tissue is fully remodeled and integrated on the scaffold. Different arrangements were designed by modifying the collection speeds of the rotating mandrel, which allowed us to obtain random, semi-aligned and mostly aligned patterns. Furthermore, dispersions of MWCNTs in polyurethane solutions were spun in the same fashion as that of pristine nanofibers, so a comparative study could be performed. The mechanical properties of nanofibers showed an increase with higher fiber alignment, as well as with the incorporation of MWCNTs. In addition, the morphological appearance of cells grown on nanofibers indicates that cells grow along the nanofiber direction.

Experimental

Material synthesis

Medical grade polyurethane Tecoflex® EG-80A was kindly donated by Lubrizol Advanced Materials, Inc. Tetrahydrofuran (THF, 99+%) and N, N-dimethylformamide (DMF, 99.8%) were purchased from Sigma-Aldrich, (USA); these solvents were used without further purification. Baytubes® C 150 P (MWCNTs) were a gift from Bayer Materials. Dulbecco's Modified Eagle's Medium (DMEM, ATCC) supplemented with a 10% fetal calf serum was purchased from Invitrogen (Grand Island, NY). NIH 3T3 mouse fibroblast cells were purchased from ATCC (CRL-1658™). Penicillin/Streptomycin (Gibco™), 0.4% Trypan Blue dye (Invitrogen), 96 wells microplates (Corning, NY), Glycine buffer (0.1M glycine from Bio-Rad, Plus 0.1M NaCl from Sigma and equilibrated to pH 10.5 with 0.1N NaOH) were used as received.

Preparation of polymeric solutions

Electrospinning of polyurethane was performed using a 10 wt% solution by dissolving the polymer pellets in THF and adding DMF to reach a 1:1 solvent ratio. The polyurethane nanofibers containing MWCNTs were prepared as follows. The MWCNTs were dispersed in DMF through continuous sonication for 1 h at 50% amplitude in ultrasonic equipment (UIP1000hd Hielscher Ultrasound Technology); an ice bath was used to avoid excessive heat generated during the sonication process. The sonication process resulted in a homogeneously dispersed and stable colloid with a dark ink-like appearance and no precipitate for several hours. This MWCNTs dispersion was added to the previously dissolved polyurethane solution in THF. Through this process, dispersions of the 10 wt% polymer concentration containing 0.5 wt% MWCNTs in THF: DMF were prepared for electrospinning. The concentration of MWCNTs was selected based on a previous publication from our group, where we reported that the highest mechanical properties were reached at this concentration [**20**].

Electrospinning process

The polymer solutions and polymer-MWCNTs dispersions were injected using a 10 mL glass syringe with a 22 needle gauge (0.7mm OD×0.4mm ID) at a flow rate of 0.02 mL/min, which was controlled using a KDS 210 pump (KD Scientific Holliston, Inc., MA). The high power supply (model ES30P-5W) was purchased from Gamma High Voltage Research (Ormond Beach, FL). The positive electrode (anode) was connected to the needle tip through an alligator clip with an applied voltage of +15 kV. A negative electrode (cathode) with an applied voltage of −15 kV was attached to the grounded metallic collector. The solutions were electrospun with a 15 cm working distance (**Scheme 1**). Three different rotation speeds (798, 3240 and 5740 rpm) were used to obtain the nanofibers with different patterns. The as-spun nanofibers were vacuum dried for 24 h in the presence of P_2O_5 to remove any possible residual moisture or residual solvents.

Cell culture studies

To study the cell growth pattern on the obtained nanofibers, NIH 3T3 fibroblasts were efficiently raised from an available cryogenic vial into a 25 mL culture flask in DMEM media, which was supplemented with 10% fetal calf serum and 1% of penicillin and streptomycin in a humidified incubator at 5.2% CO_2 environment and 37°C. After obtaining 90% of confluent growth, the cell population was sub-cultured to reach a cell number of 25,000 cells/mL,which was maintained for seeding the nanofibers. Cell seeding was conducted by adding 160 µl of the 25,000 cells/mL solution to microplate wells and allowed to grow for 24 h to create a favorable environment before the nanofibers were introduced. After the initial 24 h incubation period, the media was taken out and 80 µl of fresh media was added to the wells. At this point, the nanofibers (which were previously sterilized by exposure to ethanol and/or UV light) were added to the 96 wells microplates by triplicate, and 80 µL of fresh media was added to each well in order to have a final volume of 160 µL. Finally, the microplates were incubated at 37°C with 5.2% CO_2 for 5 days, replenishing the exhausted media every 3 days.

Characterization

To investigate the morphology and alignment of nanofibers, scanning electron microscopy (SEM) was performed using an EVO® LS10 (Carl Zeiss Microscopy). The samples were coated with a thin layer of silver-palladium for 180 sec at 45mA with the Desk II Denton Vacuum Cold Sputter. After coating, the micrographs were taken at an accelerating voltage of 10.75 kV. The Raman spectra for pristine and polymer-MWCNTs nanofibers were obtained on a Bruker Optics Raman Spectrometer (BX51) at 785 nm laser excitation. The laser power density was kept as 10 mW with 50 integrations, 2 co-additions and a 25×100 nm of aperture. Spectra were collected at various locations using a microscope with 50X magnification on each sample. The thermal stability of nanofiber mats was carried out on a TGA 7 (Perkin Elmer Co., USA) by heating samples from 30° to 700°C under a continuous nitrogen purge of 20 mL/min. The heating rate was 20°C/min. The mechanical behavior of the nanofiber mats was investigated at room temperature using an INSTRON® tensile tester 5943 with a 25 N maximum load cell under a crosshead speed of 10 mm/min. Samples were cut in the form of a "dog-bone" shape via die cutting from nonwoven mats (2.75 mm wide at their narrowest point with a gauge length of 7.5 mm), following our previously established procedure [**21**]. At least five specimens were tested for tensile behavior and the average values were reported. Chemical fixation of cells was carried out in each sample after 5 days of incubation, so that the pattern of cell attachment and cell survival on the nanofibers could be determined. Therefore, nanofiber samples were rinsed twice with phosphate buffer saline (PBS) and subsequently fixed in 2.5% glutaraldehyde for 1 h. After cell fixation, samples were rinsed with distilled water and then dehydrated with graded concentrations of ethanol (20, 30, 50, 70 and 100%) for 10 min each. To remove the residual ethanol, the samples were kept in a vacuum oven for 12 h and analyzed by SEM.

Results and discussion

Fig. 1 shows the SEM images of obtained nanofibers after the electrospinning process. In these images, the prepared nanofibers show smooth, uniform, continuous, and bead-free morphologies. **Fig. 1a, b** and **c** present the pristine polyurethane nanofibers and demonstrate that higher rotation speeds (i.e., 798, 3240 and 5740 rpm, respectively) in the collector promote an increase in nanofiber alignment, transforming from random to semi-aligned to mostly aligned non-woven mats. Moreover, **Fig. 1d, e** and **f** show the SEM micrographs of nanofibers incorporating MWCNTs, where it can be observed that the addition of MWCNTs did not have an effect on nanofiber morphologies or alignments, but it did cause smaller fiber diameters. This effect has been documented in several reports, and is attributed to an increase in the solution's electrical conductivity by the addition of MWCNTs, which leads to thinner nanofibers [**34, 35**].

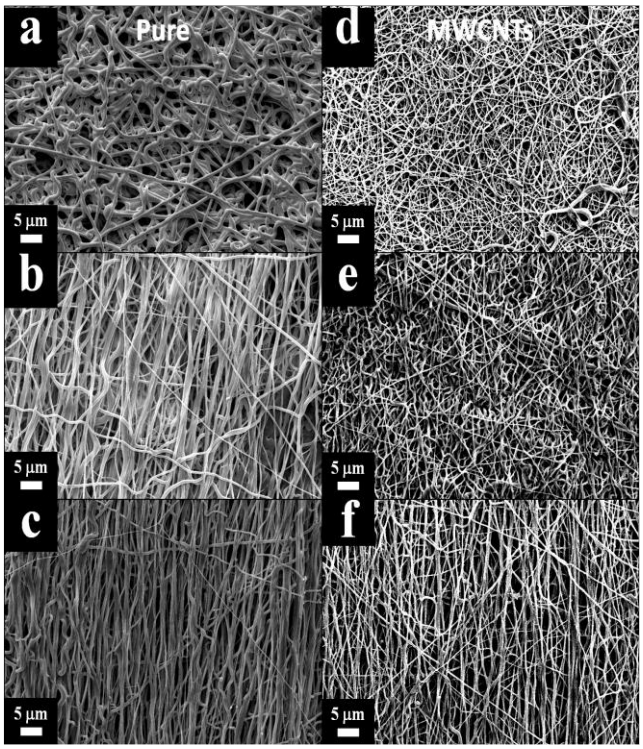

Fig. 1. SEM micrographs of obtained nanofibers showing the formation of completely aligned nanofibers by increasing the rotation speeds of the collector. Pure polyurethane nanofibers after running the samples with rotation speeds of 798 rpm (a), 2340 rpm (b) and 5740 rpm (c). Polyurethane nanofibers containing MWCNTs after running the samples with rotation speeds of 798 rpm (d), 3240 rpm (e) and 5740 rpm (f).

Fig. 2a shows the Raman spectra of pristine polyurethane nanofibers. It is observed that the peaks positioned at 2913 cm^{-1}, 2856 cm^{-1} and 2794 cm^{-1} correspond to aliphatic CH_2 stretching in pristine nanofibers. Peaks at 1436 cm^{-1} and 1485 cm^{-1} are due to aliphatic CH_2 bending, 1296 cm^{-1} for C-N stretching, while peaks at 1033 cm^{-1} and 1114 cm^{-1} are assigned to aliphatic asymmetric C-O-C stretching, and the peak at 834 cm^{-1} is assigned to N-H wagging from the polymer backbone **[36]**. All the patterns (random, semi-aligned and mostly aligned) show the same peaks, with slight variations in their relative

intensities. Incorporation of MWCNTs suppresses the detection of polymer peaks, so the only peaks observed correspond to the carbon nanotubes due to higher scattering (**Fig. 2b**). The inset in figure 2b presents the Raman spectrum of pristine MWCNTs, showing the peaks at 1307 cm^{-1} and 1604 cm^{-1}, which correspond to vibrations, caused by the disordered induced D-band and the tangential G-band respectively [**37**], the relative heights of the bands indicate that the MWCNTs contain significant amounts of defects and disordered regions. These vibrations are also present in the spectra of the nanofibers containing MWCNTs for the random, semi-aligned and mostly aligned arrangements. The D-band appears at 1312 cm^{-1}, 1314 cm^{-1} and 1314 cm^{-1} respectively, and the G-band appears at 1610 cm^{-1}, 1599 cm^{-1} and 1599 cm^{-1}. The shift to higher frequencies in the D-band indicates the interaction between the polymer matrix and the MWCNTs, which suggest that the polymer around the outermost MWCNTs layers constrains them, and thus higher energy is required for this material to vibrate [**38, 39**].

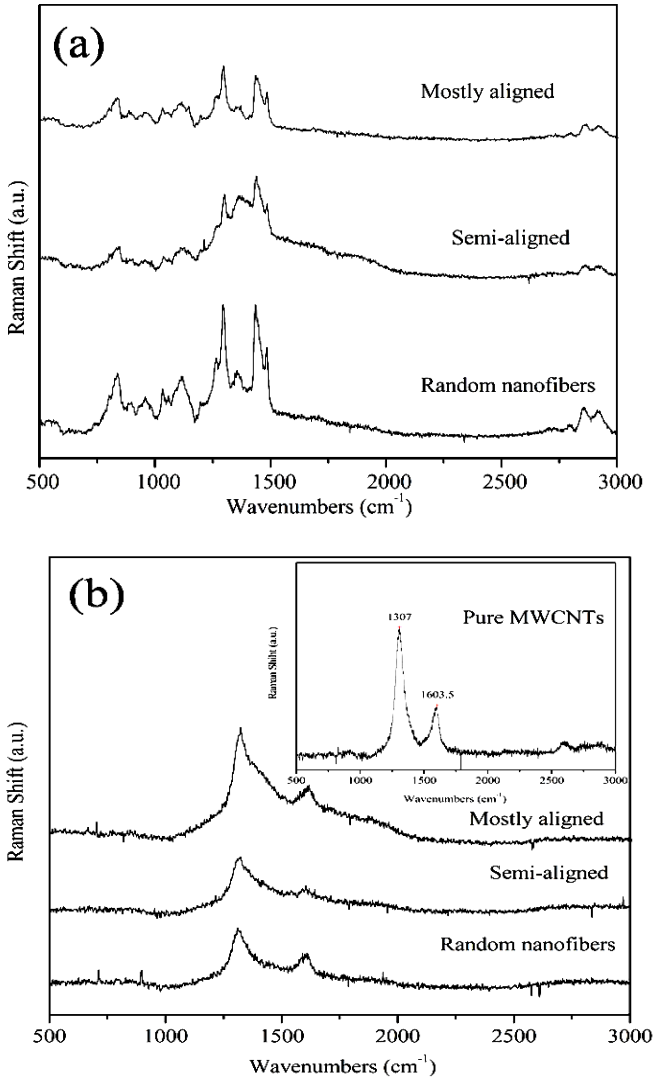

Fig. 2. (a) Raman spectra of pristine polyurethane nanofibers and (b) raman spectra of the nanofibers containing MWCNTs. The inset shows the Raman spectrum of pristine MWCNTs.

Fig. 2c shows the TGA analysis of pristine nanofibers. This figure shows that the onset decomposition temperatures of random nanofibers was 316°C, 313°C for semi-aligned, and 311°C for mostly aligned nanofibers. However, the random nanofibers have a higher weight loss before the decomposition step starts. Moreover, the random nanofibers decompose in two steps, while the semi-aligned and mostly aligned patterns decompose in one step. **Fig. 2d** shows the TGA graphs of nanofibers containing MWCNTs, where a similar decreasing pattern in the onset decomposition temperatures was evident, 344°C for random, 329°C for semi-aligned and 322°C for mostly aligned. The presence of MWCNTs within the nanofibers caused an increase in the onset temperature of these fibers when compared to their analogous without MWCNTs, while presenting a single decomposition step.

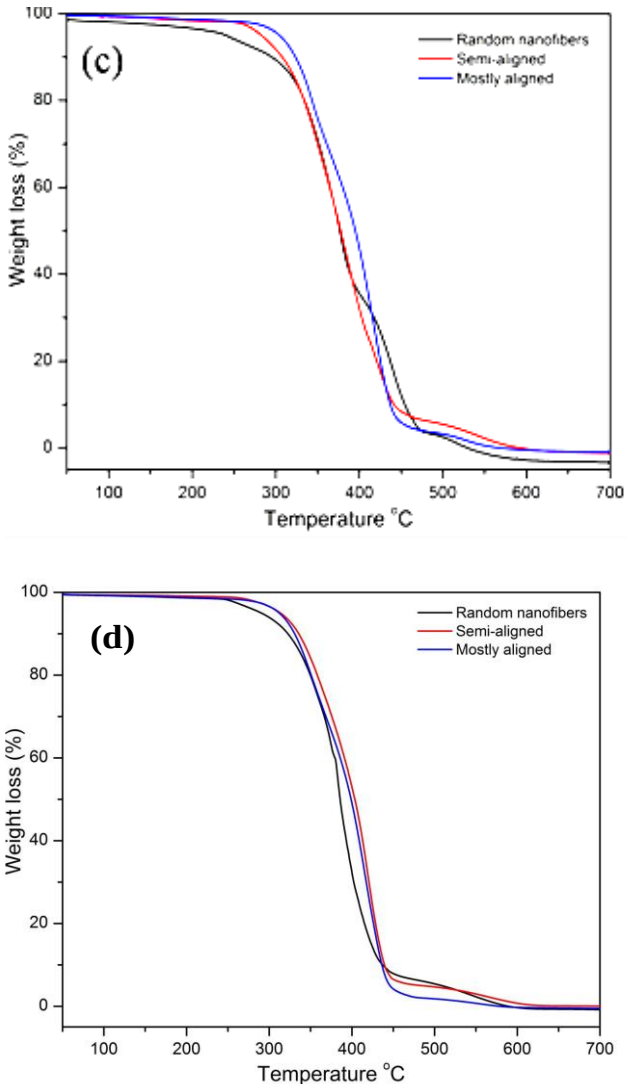

Fig. 2. Thermogravimetric analysis of (c) pristine polyurethane nanofibers and (d) nanofibers containing MWCNTs.

Fig. 3a and b show the stress vs. strain curves for pristine nanofibers and nanofibers-MWCNTs respectively. In these figures, we can observe that while collection speeds increased, thus promoting the subsequent change from random to semi-aligned to mostly aligned, the tensile

stress increased and the elongation decreased. Moreover, **Fig. 3c** presents the bar graphs of the average tensile stress showed by the nanofibers, confirming the increase in the mechanical properties of pristine nanofibers from 23 ± 1.3 to 39 ± 8.1 MPa, and an even larger increase in nanofibers containing MWCNTs from 27 ± 2.7 to 39 ± 1.3 MPa.

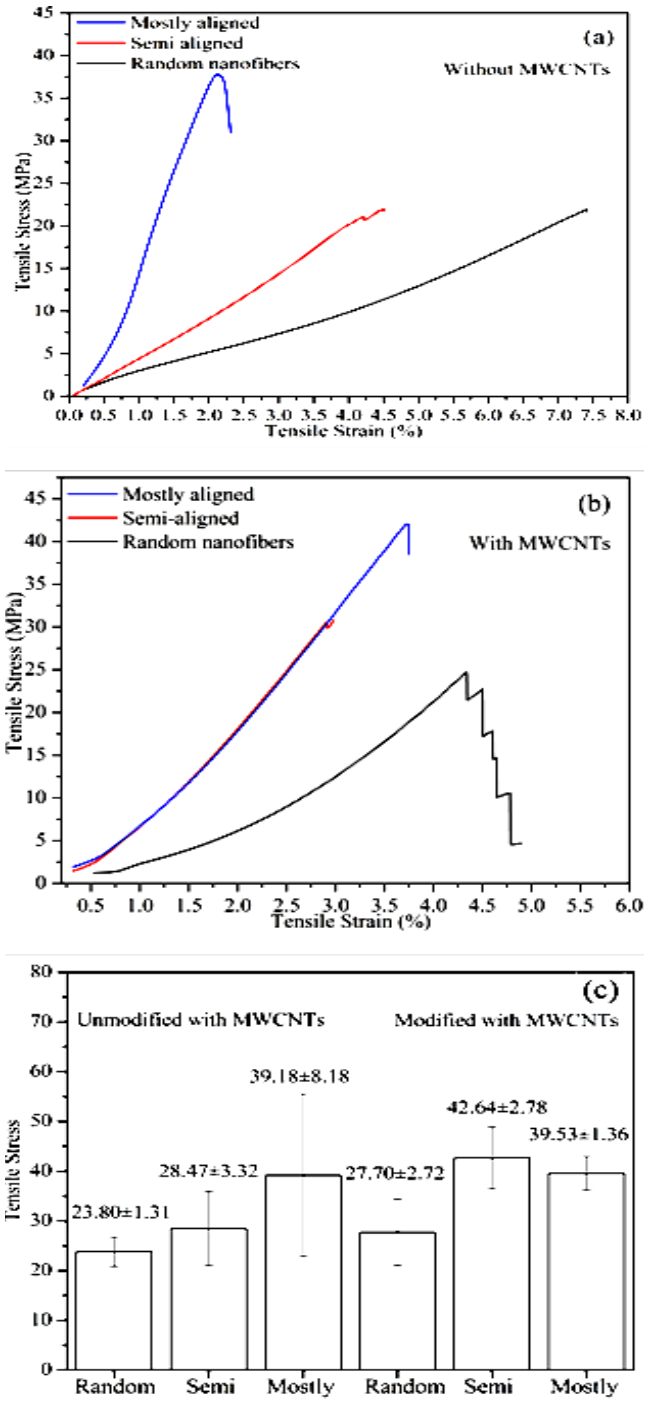

Fig. 3. Stress vs. strain curves of the pristine nanofibers with different collector rotational speeds, resulting in random, semi-aligned and mostly aligned patterns (a), Stress vs. strain curves of the nanofibers containing MWCNTs with different collector rotational speeds, resulting in random, semi-aligned and mostly aligned patterns (b) and bar graphs showing the average tensile stress of nanofibers with and without MWCNTs (c).

Fig. 4 shows the SEM micrographs of the nanofibers after cell fixation, suggesting that the cells attached to the nanofiber mats. In these images (**Fig. 4a and d**), which consist of nanofibers with random patterns, we observe that cell growth proceeded without any particular direction, similar to previous reports [**15, 40**]. It is also observed that these cells possess a round morphology (**Fig. 4a and d**), which is indicative of stressful behavior. However, as the nanofibers aligned, due to the increase in collection speeds, the cells followed and grew along the nanofiber direction, and exhibited an elongated morphology (**Fig. 4c and f**), also appearing to have penetrated the fibers, so as to form cell buds. The growth along the nanofiber axis is in perfect agreement with guided tissue regeneration patterns [**41, 42**].

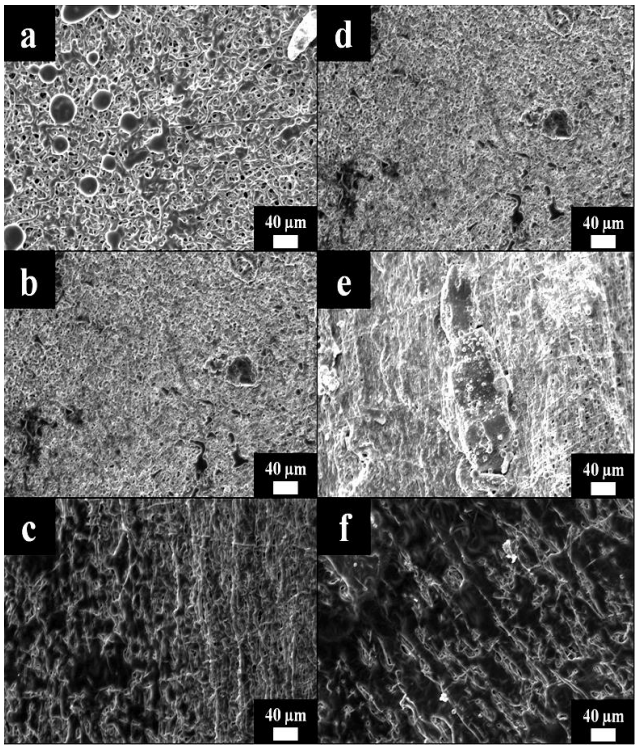

Fig. 4. SEM micrographs of nanofibers after cell fixation test. Nanofibers without MWCNTS, randomly aligned (a), semi-aligned (b) and mostly aligned (c). Nanofibers with MWCNTS, randomly aligned (d), semi-aligned (e) and mostly aligned (f).

Conclusion

In conclusion, different nanofiber patterns can be produced by increasing the rotation speeds of the collector. The rotational speeds used (798, 3240 and 5740 rpm) led to random, semi-aligned and mostly aligned patterns of non-woven mats, respectively. Raman spectroscopy confirmed the presence of MWCNTs embedded within the nanofibers, which caused an enhancement on the thermal stability of the material. Further, the mostly aligned nanofiber pattern presented the higher tensile strength of the material. Finally, cell culture studies were used to determine the cell growth patterns on nanofibers, indicating that the mostly aligned non-woven mats guide cell growth and direction.

Acknowledgements
The authors wish to acknowledge Mr. Joseph D. Ventura from Bayer Materials Science for providing the Multiwalled Carbon Nanotubes used

in these studies, and Raul Salazar from Lubrizol Advanced Materials for providing Tecoflex® EG-80A.

Reference

1. Laurencin, C.T.; Ambrosio, A.M.; Borden, M.D.; Cooper, J.A.; *Annu; Rev. Biomed. Eng* **1999**, *1*, 19. **DOI:** 10.1146/annurev.bioeng.1.1.19
2. Hollister; S.J. Nat Mater. **2005**, 4, 518. **DOI:** 10.1038/nmat1421
3. Chan, B.P.; Leong, K.W.; *Eur Spine J*. **2008**, *17*, 467. **DOI:** 10.1007/s00586-008-0745-3
4. Discher, D.E.; Janmey, P.; Wang, Y.L.; *Science*. **2005**, *310*, 1139. **DOI:** 10.1126/science.1116995
5. Formhals, A.; Richard, S.G. U.S. Patent 1975504 A, **1934**.
6. Formhals, A. U.S. Patent 2158415A, **1939**.
7. Formhals, A. U.S. Patent 2187306A, **1940**.
8. Formhals, A. U.S. Patent 2323025A, **1943**.
9. Formhals, A. U.S. Patent 2349950A, **1944**.
10. Taylor, G.; P.*Roy Soc Lond A Mat*, **1964**, *280*, 383.
11. Taylor G.; Electrically Driven Jets. P *Roy Soc Lond A Mat*, **1969**, *313*, 453.
12. Kondawar, S.B.; Patil, P.T.; Agrawal, S.P.; *Adv. Mat .Lett*. **2014**, *5*, 389. **DOI:** 10.5185/amlett.2014.amwc.1037
13. Dhakate, S.R.; Singla, B.; Uppal, M.; Mathur, R.B.; *Adv. Mat .Lett.* **2010**, *1*, 200. **DOI:** 10.5185/amlett.2010.8148
14. Luis, D.-G.; Alvarez-Lorenzo, C.; Concheiro, A.; Silva, M.; Dominguez, F.; Sheikh, F.A.; Cantu, T.; Desai, R.; Garcia, V.L.; Macossay, J. *J., Mater. Sci. Eng., C*. **2014**, *40*, 180. **DOI:** 10.1016/j.msec.2014.03.065
15. Dhakate, S.R.; Singla, B.; Uppal, M.; Mathur, R.B.; *Adv. Mat .Lett.* **2010**, *1*, 200. **DOI:** 10.5185/amlett.2010.8148
16. Zdrahala, R.J.; *J Biomater Appl.* **1999**, *14*, 67. **DOI:** 10.1177/088532829901400104
17. Boretos, J.W.; *Past, Pure & Appl. Chem*; **1980**, *52*, 1851. **DOI:** 10.1351/pac198052071851
18. Gogolewski S.; *Colloid Polym. Sci* **1989**, *267*, 757. **DOI:** 10.1007/BF01410115
19. Kidoaki, S.; Kwon, I.K.; Matsuda, T.; *J Biomed Mater Res Part B*. **2006**, *76B*, 219. **DOI:** 10.1002/jbm.b.30336
20. Macossay, J.; Sheikh, F.A.; Cantu, T.; Eubanks, T.M.; Salinas, M.E.; Farhangi, C.S.; Ahmad, H.; Shamshi, H.M.; Khil, M.S.; Maffi, S.K.; Kim, H.; Bowlin, G.L.; *Appl. Surf. Sci*. **2014**, *321*, 205. **DOI:** 10.1016/j.apsusc.2014.09.198
21. Sheikh, F.A.; Ju, H.W.; Moon, B.M.; Park, H.J.; Kim, J.-H.; Kim, S.H.; Lee, O.J.; Park, C.H. *J. Bioact. Compat. Polym.* **2014**, *29*, 500. **DOI:** 10.1177/0883911514549717
22. Salvetat, J.P.; Bonard, J.M.; Thomson, N.H.; Kulik, A.J.; Forró, L.; Benoit, W.; Zuppiroli, L. *Appl. Phys. A*; **1999**, *69*, 255. **DOI:** 10.1007/s003399900114
23. Salvetat, J.P.; Rubio, A. *Carbon*; **2002**, *40*, 1729. **DOI:** 10.1016/S0008-6223(02)00012-X
24. Ajayan P.M. *Chem. Rev*; **1999**, *99*, 1787. **DOI:** 10.1021/cr970102g
25. Ajayan, P.M.; Schadler, L.S.; Giannaris, C.; Rubio, A. *Adv. Mater*. **2000**, *12750*, 753. **DOI:** 10.1002/(SICI)1521-4095(200005)12:10<750::AID-ADMA750>3.0.CO;2-6
26. Matthias, M.; Arnim, S.; Yogendra, K.M.; Sören, K.; Rainer, A.; Andriy, L.; Lorenz, K.; Karl.; *S. Adv. Mater*. **2012**, *24*, 3486. **DOI:** 10.1002/adma.201200491
27. Ebbesen, T.W.; Ajayan, P.M.; *Nature*. **1992**, *358*, 220. **DOI:** 10.1038/358220a0
28. Ajayan, P. M.; Stephan, O.; Colliex, C.; Trauth,D.; *Science*. **1994**, *265*, 1212. **DOI:** 10.1126/science.265.5176.1212
29. Chłopek, J.; Czajkowska, B.; Szaraniec, B.; Frackowiak, E.; Szostak, K.; Béguin, F. *Carbon*. **2006**, *44*, 1106. **DOI:** 10.1016/j.carbon.2005.11.022
30. Smart, S.K.; Cassady, A.I.; Lu, G.Q.; Martin, D.J.; *Carbon*. **2006**, *44*, 1034. **DOI:** 10.1016/j.carbon.2005.10.011
31. Joseph, W.F.; Mia, D.W.; Damond A.C.; Emmanuel, C.E.; Tea A.; Emmanuel, A.A.; Christian, H.B.; Cato, T.L.; *J. Biomech*. **2011**, *44*, 694. **DOI:** 10.1016/j.jbiomech.2010.10.043
32. Joseph, W.F.; Mia, D.W.; Cato, T.L.; *J. Biomech*. **2007**, *40*, 2029. **DOI:** 10.1016/j.jbiomech.2006.09.025
33. Luis, D.-G.; Florencia, M.B.; Gustavo, A.A.; Angel, C.; Carmen, A-L. J. *Appl. Polym. Sci*. **2015**, *132*, 41372. **DOI:** 10.1002/app.41372
34. Macossay, J.; Ybarra, A.V.R.; Arjamend, F.A.; Cantu, T.; Eubanks, T.M.; Chipara, M.; López-Cuéllarg, E.; Nasser, M-N. *Des. Monomers Polym*; **2012**, *15*, 197. **DOI:** 10.1163/156855511X615065
35. Chipara, D.M.; Macossay, J.; Ybarra, A.V.R.; Chipara, A.C.; Eubanks, T.M.; Chipara, M. *Appl. Surf. Sci;* **2013**, *275*, 23. **DOI:** 10.1016/j.apsusc.2013.01.116
36. Janik, H.; Pałys, B.; Petrovic, Z.S. *Macromol. Rapid Commun;* **2003**, *24*, 265. **DOI:** 10.1002/marc.200390039
37. Zheng, X.; Xu, Q.; *J. Phys. Chem*. C. **2010**, *114*, 9435. **DOI**: 10.1021/jp103932b
38. Liu, A.; Honma, I.; Ichihara, M.; Zhou, H.; Haoshen, Z. *Nanotechnology*. **2006**, *17*, 2845. **DOI:** 10.1088/0957-4484/17/12/003
39. Yadav, S.K.; Mahapatra, S.S.; Yoo, H.J.; Cho, J.W.; *Nanoscale Res. Lett*. **2011**, *6*, 122. **DOI:** 10.1186/1556-276X-6-122
40. Bhattarai, S.R.; Bhattarai, N.; Yi, H.K.; Pyong, H.H.; Chad, D.I.; Kim, H.Y.; *Biomaterials.* **2004**, *25*, 2595. **DOI:** 10.1016/j.biomaterials.2003.09.043
41. Xua, C.Y.; Inai, R.; Kotaki, M.; Ramakrishna, S; *Biomaterials*. **2004**, *25*, 877. **DOI:** 10.1016/S0142-9612(03)00593-3
42. Xue, J.; He, M.; Liu, H.; Niu, Y.; Crawford, A.; Coates, PD.; Chen, D.; Shi, R.; Zhang, L.; *Biomaterials.* **2014**, *35*, 9395. **DOI:** 10.1016/j.biomaterials.2014.07.060